Original Paper

Cerebrovascular Diseases

Cerebrovasc Dis 2014;38:344–353
DOI: 10.1159/000368597

Received: June 16, 2014
Accepted: September 23, 2014
Published online: November 21, 2014

Microvascular Plasticity After Experimental Stroke: A Molecular and MRI Study

Anaick Moisan[a–c] Isabelle M. Favre[a, b, d] Claire Rome[a, b] Emmanuelle Grillon[a, b] Bernadette Naegele[a, b, d] Marianne Barbieux[a, b, d] Florence De Fraipont[e, f] Marie-Jeanne Richard[c, e, f] Emmanuel L. Barbier[a, b] Chantal Rémy[a, b] Olivier Detante[a, b, d]

[a]Inserm, U836, [b]University Grenoble Alpes, GIN, Grenoble, [c]French Blood Company/Grenoble University Hospital, Cell Therapy and Engineering Unit, Saint Ismier, [d]Grenoble University Hospital, Stroke Unit, Department of Neurology, [e]Inserm, U823, University Grenoble Alpes, Institut Albert Bonniot, and [f]Grenoble University Hospital, Cancer Biochemistry and Biotherapies, Grenoble, France

Key Words

Cerebral ischemia · Angiogenic factors · Angiogenesis · Microvascular MRI · Stroke · Pathophysiology · Microvasculature · Vessel size index · Brain plasticity

Abstract

Background: Microvasculature plays a key role in stroke pathophysiology both during initial damage and extended neural repair. Moreover, angiogenesis processes seem to be a promising target for future neurorestorative therapies. However, dynamic changes of microvessels after stroke still remain unclear, and MRI follow-up could be interesting as an in vivo biomarker of these. ***Methods:*** The aim of this study is to characterize the microvascular plasticity 25 days after ischemic stroke using both in vivo microvascular 7T-MRI (vascular permeability, cerebral blood volume (CBV), vessel size index (VSI), vascular density) and quantification of angiogenic factor expressions by RT-qPCR in a transient middle cerebral artery occlusion rat model. CBV and VSI (perfused vessel caliber) imaging was performed using a steady-state approach with a multi gradient-echo spin-echo sequence before and 2 min after intravenous (IV) injection of ultrasmall superparamagnetic iron particles. Vascular density (per mm^2) was derived from the ratio $[\Delta R_2/(\Delta R_2^*)^{2/3}]$. Blood brain barrier leakage was assessed using T_1W images before and after IV injection of Gd-DOTA. Additionally, microvessel immunohistology was done. ***Results:*** 3 successive stages were observed: 1) 'Acute stage' from day 1 to day 3 post-stroke (D1–D3) characterized by high levels of angiopoietin-2 (Ang2), vascular endothelial growth factor receptor-2 (VEGFR-2) and endothelial NO synthase (eNOS) that may be associated with deleterious vascular permeability and vasodilation; 2) 'Transition stage' (D3–D7) that involves transforming the growth factors β1 (TGFβ1), Ang1, and tyrosine kinase with immunoglobulin-like and endothelial growth factor-like domains 1 (Tie1), stromal-derived factor-1 (SDF-1), chemokine receptor type 4 (CXCR-4); and 3) 'Subacute stage' (D7–D25) with high levels of Ang1, Ang2, VEGF, VEGFR-1 and TGFβ1 leading to favorable stabilization and maturation of microvessels. In vivo MRI appeared in line with the angio-

A.M. and I.M.F. contributed equally to the manuscript.

1015–9770/14/0385–0344$39.50/0

E-Mail karger@karger.com
www.karger.com/ced

Dr. Olivier Detante
Stroke Unit, Neurology
CHU Grenoble, CS 10217
FR–38043 Grenoble (France)
E-Mail ODetante@chu-grenoble.fr

genic factors changes with a delay of at least 1 day. All MRI parameters varied over time, revealing the different aspects of the post-stroke microvascular plasticity. At D25, despite a normal CBV, MRI revealed a limited microvessel density, which is insufficient to support a good neural repair. ***Conclusions:*** Microvasculature MRI can provide imaging of different states of functional (perfused) microvessels after stroke. These results highlight that multiparametric MRI is useful to assess post-stroke angiogenesis, and could be used as a biomarker notably for neurorestorative therapy studies. Additionally, we identified that endogenous vessel maturation and stabilization occur during the 'subacute stage'. Thus, pro-angiogenic treatments, such as cell-based therapy, would be relevant during this subacute phase of stroke.

Introduction

Stroke is the second leading cause of death worldwide and the first cause of disability. Except management in stroke care units including rehabilitation, early thrombolysis or intake of aspirin, and encouraging results of preliminary trials related to serotonin reuptake inhibitors [1], no effective treatment exists to improve functional recovery beyond the first hours. As all clinical trials focused on neuroprotection failed, other targets are being investigated. Aside neurogenesis, apoptosis, and inflammation processes [2], angiogenesis plays a key role during neural repair [3, 4], and is a promising target for future neurorestorative therapies [5]. Angiogenesis has been related to neuronal survival and functional recovery in humans and animals [6, 7]. Currently, one should rather consider the 'glio-neurovascular unit' such as the functional integration of EC, astrocytes, neurons, and extracellular matrix (ECM) [8]. After stroke, cell–cell signaling within this glio-neurovascular unit is altered, mediating acute and subacute events over hours to months [9–18], as reviewed by Beck and Plate at a molecular level [19]. In this review, authors however acknowledge that data arises from different animal models (e.g., transient or permanent occlusion in rat or mice).

In vivo, a longitudinal analysis of cerebral microvasculature changes may be monitored using magnetic resonance imaging (MRI) at preclinical and clinical levels [20]. Data have been collected using a transient (60 min) three-vessel occlusion model in rats [21], a permanent embolic stroke model in rats [22, 23], and a transient (60 min) intraluminal occlusion model in rats [24].

It thus appears of interest to characterize if a relation could be established between molecular changes and microvascular changes observed in vivo by MRI after stroke. More specifically, is MRI sensitive to the angiogenic molecular events? What is the delay between angiogenic molecular changes and microvascular changes? In the present study, we monitored microvascular changes at a molecular level – using biological assays – and at an integrated level – using microvascular MRI in a transient (90 min) stroke model in rats (n = 47) during 25 days.

Material and Methods

All animal procedures were run according to the French laws (permits 381106 for AM, 380820 for CR and A3851610008 for experimental and animal care facilities) with the approval of the local ethical committee (agreement number 004). Anesthesia was induced by inhalation of 5% isoflurane (Abbott Scandinavia AB, Solna, Sweden) in 30% O_2 in air and maintained with 2–2.5% isoflurane through a facial mask (for surgical and imaging procedures). Rectal temperature was monitored and maintained at 37.0 ± 0.5°C.

Abbreviations used in this article

αSMA	Alpha smooth muscle actin	IV	Intravenous
Ang1	Angiopoietin 1	MCAo	Middle cerebral artery occlusion
Ang2	Angiopoietin 2	mNSS	Modified neurological severity score
ART	Adhesive removal test	ROI	Region of interest
BBB	Blood brain barrier	SDF-1	Stromal-derived factor-1
CBV	Cerebral blood volume	TGFβ1	Transforming growth factor β1
CXCR-4	Chemokine receptor type IV	USPIO	Ultrasmall superparamagnetic iron oxide
EC	Endothelial cell	VEGF	Vascular endothelial growth factor
ECM	Extracellular matrix	VEGF-R1	Vascular endothelial growth factor – receptor 1
eNOS	Endothelial nitric oxide synthase	VEGF-R2	Vascular endothelial growth factor – receptor 2
FGF-2	Basic fibroblast growth factor	VSI	Vessel size index
IC	Intracerebral	vWF	von Willebrand factor

Transient Middle Cerebral Artery occlusion (MCAo) Model and Experimental Groups

Forty seven male Sprague Dawley rats weighing 280–330 g (7–8 weeks old) underwent a surgery at D0. Animals were randomly allocated to the MCAo or sham group. In 34 rats, a 90 min-focal brain ischemia was induced by intraluminal occlusion of the right MCA (MCAo) (silicon rubber-coated monofilaments: 0.37 mm diameter, Doccol Corp., Sharon, Mass., USA) according to our previously described method [25–27]. Hemorrhagic and partial lesions (only striatal or cortical) were excluded from our study. Thirteen sham-operated rats underwent the same surgery without MCA occlusion. Eight MCAo and 9 sham rats were followed during 25 days for behavior and MRI analysis. At days 1, 2, 3, 7, 16, and 25, three MCAo rats were anesthetized and beheaded for RT-qPCR analysis. Immunohistochemistry was realized on the brains of two MCAo rats at D3, D7, D16, and D25.

In vivo MRI Experiments

Based on a previous study where microvascular events were detected up to 3 weeks after MCAo [25], MRI sessions (7T, Bruker Avance III, MRI facility of Grenoble IRMaGe) were set at D3, D7, D16, and D25. Breath rate was maintained constant between animals during each MRI session by adjusting the anesthesia level. All MRI data were acquired with the same positions and the same geometrical characteristics. T_2 weighted (T_2W) images (TR/TE = 2,500/60 ms, voxel size = 234 × 234 × 1,000 μm) were acquired to measure volume lesion. Cerebral blood volume (CBV) and VSI (perfused vessel caliber) imaging were performed using a steady-state approach. Briefly, a multi gradient-echo spin-echo sequence (TR = 4,000 ms, spin-echo = 40 ms; seven gradient-echoes from 2.3 to 15.6 ms; voxel size: 234 × 234 × 1,000 mm^3; seven slices) was applied, 2 min before and after intravenous (IV) injection of an intravascular ultrasmall superparamagnetic iron particles (USPIO, P904®, Guerbet, Roissy, France; 200 μmol iron/kg body weight). BBB leakage was assessed using T_1W images (TR/TE = 300/4.8 ms) acquired 3 min before and after IV injection of 0.2 mmol/kg Gd-DOTA (Dotarem®, Guerbet). For technical reasons, data were available from 7–8 MCAo rats and 8–9 sham rats at D3, D7 and D16, and 4 MCAo rats and 6 sham rats at D25.

The region of interest (ROI) corresponding to the whole ischemic lesion was manually delineated by a blinded operator on T_2W images, as previously described [25]. In sham rats, the ipsilateral ROI was drawn to obtain a mean ipsilateral volume equal to the mean lesion volume of the MCAo group for each MRI session.

CBV and VSI maps were computed using home-made software within Matlab (MathWorks, Natick, Mass., USA). Vascular density per mm^2 was derived from the ratio $[\Delta R_2/(\Delta R_2^*)^{2/3}]$ according to equation 7 of Wu et al. [28]. CBV, VSI, and vascular density were measured in the same ROI, from non-excluded pixels (voxels were excluded in case of erroneous fitting (CBV <0%) or when outside the range of validity of the method, i.e., CBV >17%, VSI >50 μm). CBV, VSI, and vascular density only reflect the functional vessels. BBB permeability was calculated on the T_1W images as the signal enhancement (SE, %) induced by Gd-DOTA extravasation.

Behavioral Tests

Behavioral tests were carried out by a blind operator at D2, D6, D15, and D22 after surgery on the 8 MCAo rats and the 9 shams followed by MRI. The modified Neurological Severity Score (mNSS) assessed walk, placing, and beam balance (0: no deficit, 18: highest deficit). Adhesive Removal Test (ART) was used to assess the asymmetry in dexterity and sensitivity. An adhesive paper was applied on each forelimb and the time of their removal was noted (maximum delay of 120 s). All rats were trained for 3 days before surgery (3 trials per day for each test).

SYBRGreen Real-Time RT-qPCR

To measure the expression level of genes of interest at D1, D2, D3, D7, D16, and D25, three additional MCAo animals were deeply anesthetized and beheaded for each time point. Three sham animals (D25) were used for reverse transcription-quantitative polymerase chain reaction (RT-qPCR) experiments and served as reference for the $2^{-\Delta\Delta CT}$ method (CT, cycle threshold). Total RNA was extracted from frozen hemispheres with TRIzol® reagent (Invitrogen, Life Technologies Ltd., Paisley, UK) using a Magnalyser (Roche Products, Indianapolis). Total RNA quantification was performed on a spectrophotometer (Nanodrop ND2000, Thermo Fisher Scientific, Wilmington, Mass., USA). Reverse transcription was performed under the conditions recommended by the manufacturer (GoScript®, Promega, Madison, Wisc., USA). Thirteen primers were designed using Primer3 program (online suppl. data 1; for all online suppl. material, see www.karger.com/doi/10.1159/000368597) and qPCR was performed on a Stratagene thermocycler® (Agilent technologies, Massy, France) using the SYBRGreen method [29]. The specificity of each PCR product was assessed using the dissociation reaction plot. Relative gene expression was calculated with the $2^{-\Delta\Delta CT}$ method, using the level of GAPDH and the expression in the 3 fake samples as normalization factors. Samples were duplicated for each gene analysis.

Immunohistochemistry

At D25, brain of one sham rat and at D3, D7, D16, and D25, brains of two additional MCAo were removed and stored at –80°C. Frozen sections (12 μm thick) were incubated overnight at 4°C with primary antibodies, washed with PBS, and incubated 1 h at room temperature with secondary antibodies. The degree of stabilization of vessels was assessed using a double staining blood vessel (von Willebrand Factor)/pericytes (alpha-smooth muscle actin). Primary antibodies against von Willebrand Factor (rabbit-anti-vWF, DakoCytomation, Glostrup, Denmark, 1:400) and alpha-smooth muscle actin (mouse-anti-αSMA, Sigma, 1:400) were employed. Secondary antibodies FITC-donkey-anti-mouse IgG (Invitrogen, Eugene, Oreg., USA, 1:500) and Rhodamine-conjugated-donkey-anti-rabbit IgG (Jackson Laboratories, West Grove, Pa., USA, 1:200) were used. Images were obtained using an epifluorescence microscope (Nikon Eclipse E600, Japan) and a CCD camera (Olympus, Rungis, France).

Statistical Analysis

Results are expressed as mean ± standard error of the mean (SEM) for RT-qPCR and behavior results. Results are expressed as mean ± standard deviation (SD) for MRI data. Paired t test was used for within-group comparison. Between-group comparison was performed using a Mann-Whitney test. A repeated measure analysis of variance was applied for behavioral data after testing the homogeneity-of-variance hypothesis (Levene-test). A p value ≤0.05 was considered significant.

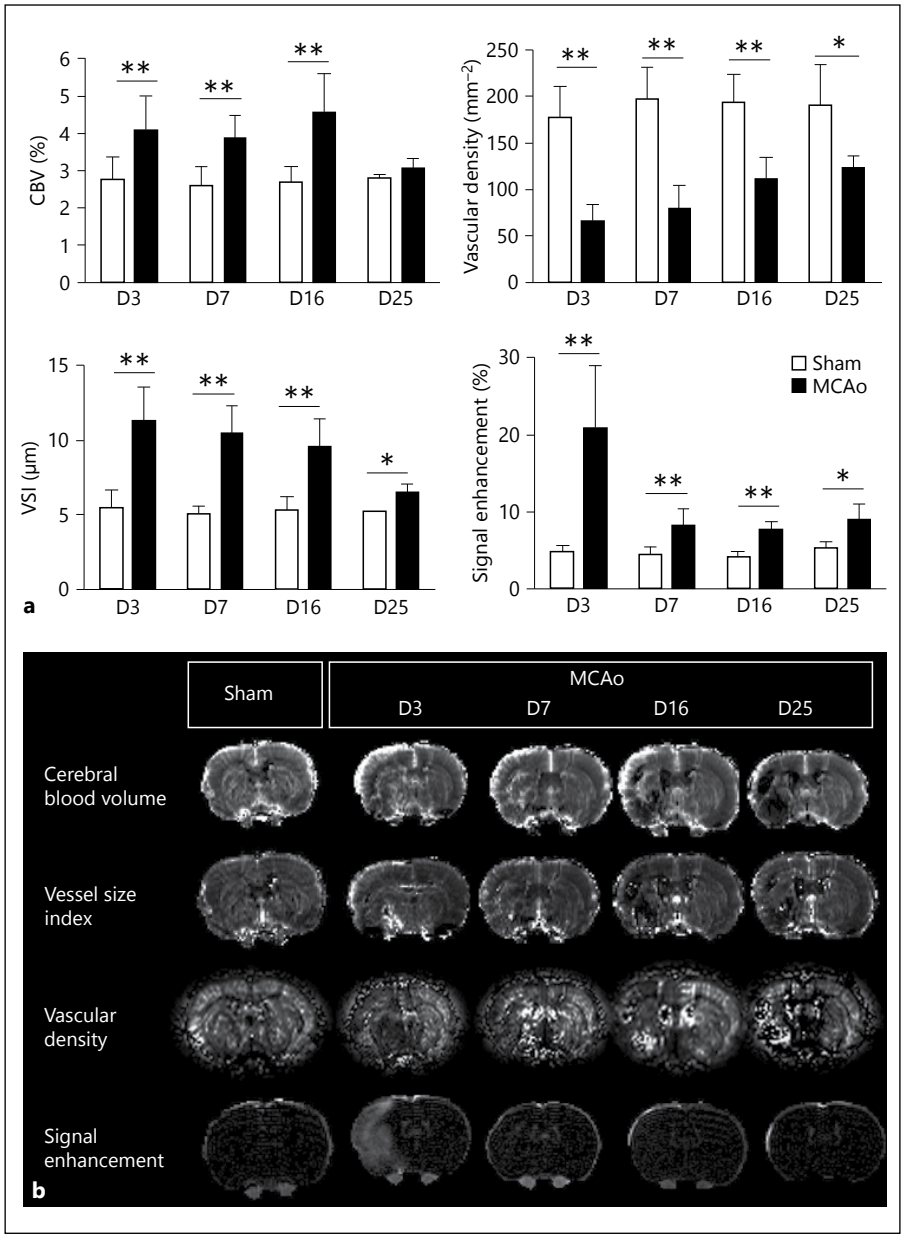

Fig. 1. a The evolution of cerebral blood volume (CBV), vessel size index (VSI), signal enhancement, and vascular density observed by MRI at D3, D7, D16, and D25 after middle cerebral artery occlusion (MCAo) into the lesion (n = 8) compared to sham rats (n = 9) (mean ± SD) with (**b**) MRI images of each parameters from a representative rat. * $p \leq 0.05$, ** $p \leq 0.01$ (Mann-Whitney).

Results

MCAo Induces a Severe Deficit at the Acute Stage with Partial Recovery Afterwards

Behavioral data and lesion volumes served as validation of our MCAo model. Cerebral lesion was confirmed in MCAo animals, which revealed higher mNSS and left forelimb ART scores compared to the shams (online suppl. data 2). The highest functional impairment was observed, two days after injury. At D25, the rats partially recovered (mNSS) but the deficit was maintained for ART. Lesions were homogeneous in volume and location between animals (the mean cortico-striatal lesion volume was maximal at D3: 223.5 ± 43.4 mm^3 with a stabilization afterwards, data not shown).

'Acute Stage' from D1 to D3: High Expression Levels of Ang2, VEGFR-2 and eNOS Precede Vasodilation and BBB Permeability

No significant changes in CBV, VSI, BBB permeability, and vascular density values were noted in sham rats during the 3 weeks (fig. 1a, b). At D3, the BBB was permeable in

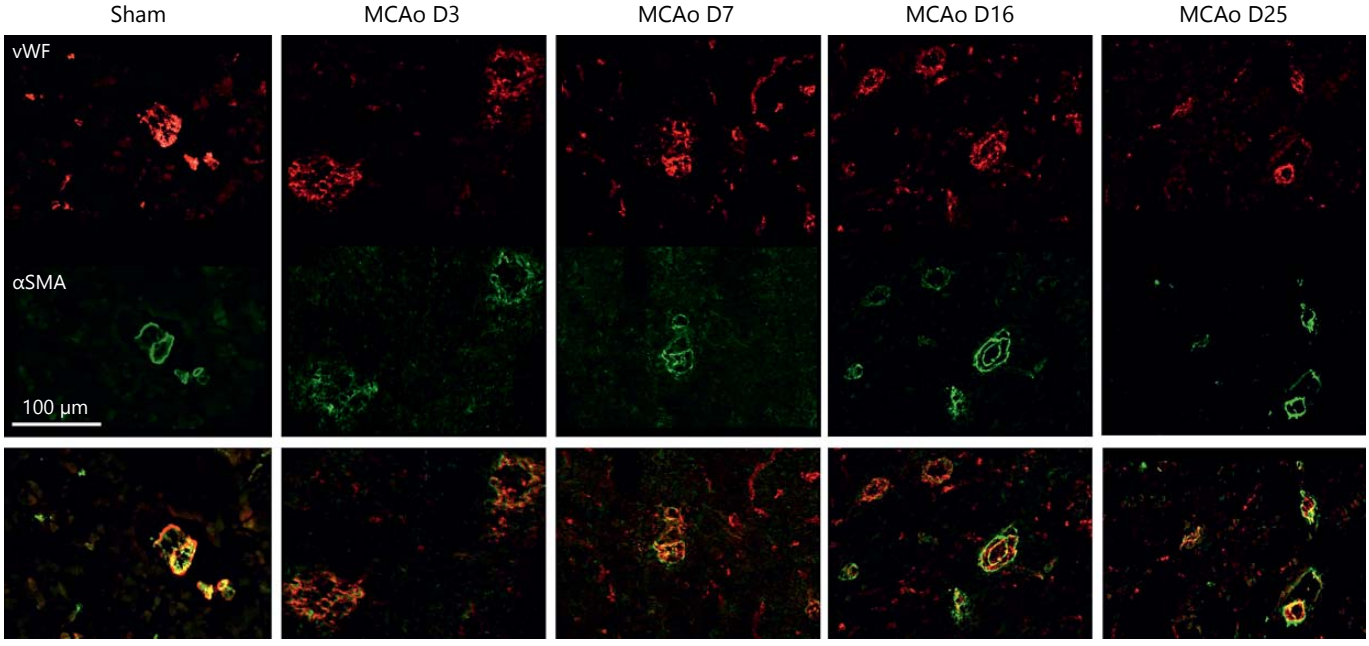

Fig. 2. Immunohistochemistry for vWF (1:400; in red for endothelial cells)/αSMA (1:400; in green for pericytes) revealing the stabilization degree of microvessels into cerebral lesion at D3, D7, D16, and D25 after middle cerebral artery occlusion (MCAo) compared to sham rats. Scale = 100 μm.

the ischemic lesion but not in sham rats (signal enhancement: 20.9 ± 8.1 vs. 5.0 ± 2.4%, p = 0.003). VSI was higher in MCAo than in sham rats at D3 (11.3 ± 2.3 vs. 5.6 ± 0.9 μm, p = 0.001). This early vasodilation compensated the decrease in vascular density observed at D3 (MCAo vs. sham: 65.7 ± 18.1 vs. 177.8 ± 33.4 mm^{-2}, p = 0.001), resulting in a higher CBV in MCAo rats than in shams (4.1 ± 0.9 vs. 2.7 ± 0.6%, p = 0.01). Consistent with MRI results, histology at D3 in MCAo rats revealed enlarged vessels with a chaotic and disorganized appearance of the surrounding αSMA-positive cells (fig. 2). At a molecular level, an overexpression of eNOS, VEGFR-2, and Ang2 was observed at D1 and D2 in MCAo brains. Compared to sham animals, the expressions of TGFβ1 and CXCR-4 were, respectively increased at D1–D3 and that of Tie1 peaked at D3. Conversely, Ang1 was underexpressed at D1 and SDF-1 at D1–D3, compared to sham animals (fig. 3).

'Subacute Stage' from D7 to D25: Increased Expression Levels of Ang1, Ang2, CXCR-4 and TGFβ1 Accompany the Raise of Vascular Density and the Decrease of Vessel Caliber

From D7 to D25, a minor BBB permeability was observed in the lesion of MCAo group compared to sham (SE at D7: 8.2 ± 2.2 vs. 4.4 ± 1.0%, p = 0.003; D16: 7.7 ± 1.0 vs. 4.3 ± 0.4%, p = 0.003; D25: 9.1 ± 2.0 vs. 5.4 ± 0.8%, p = 0.014). In MCAo rats, MRI showed a continuous decrease in vessel caliber and an increase in vascular density from D3 to D25 without reaching the sham level at D25 (VSI at D3 vs. D25: 11.3 ± 2.3 vs. 6.5 ± 0.5 μm, p = 0.003; vascular density at D3 vs. D25: 65.7 ± 18.1 vs. 123.7 ± 13.1 mm^{-2}, p = 0.013). CBV remained stable from D3 to D16 and strongly decreased to reach the sham level at D25 (CBV at D16 vs. D25: 4.5 ± 1.0 vs. 3.0 ± 0.2%, p = 0.025). In agreement with MRI data, the vessel caliber observed by histology at D16 and D25 appeared smaller than at D3 with a reorganization of αSMA-positive cells around vessels (fig. 2).

At a molecular level, Ang1 was overexpressed at D7 and Ang2 at D25. Tie1 and CXCR-4 were still overexpressed at D7. A return to baseline values was observed at D7 for eNOS and SDF-1 and at D16 for VEGF and VEGFR-1. TGFβ1 remained overexpressed after D7 compared to sham with a decrease until D25 (fig. 3).

Growth Factors Follow Different Time Courses

During the entire follow-up, no significant difference in the levels of FGF-2 and Tie2 was observed between MCAo and sham rats (fig. 3). The molecular analysis of the other factors highlighted two distinct profiles (fig. 3).

Three factors (Ang2, VEGF, and VEGFR-1) exhibited a biphasic evolution in a period of 25 days. Levels of ex-

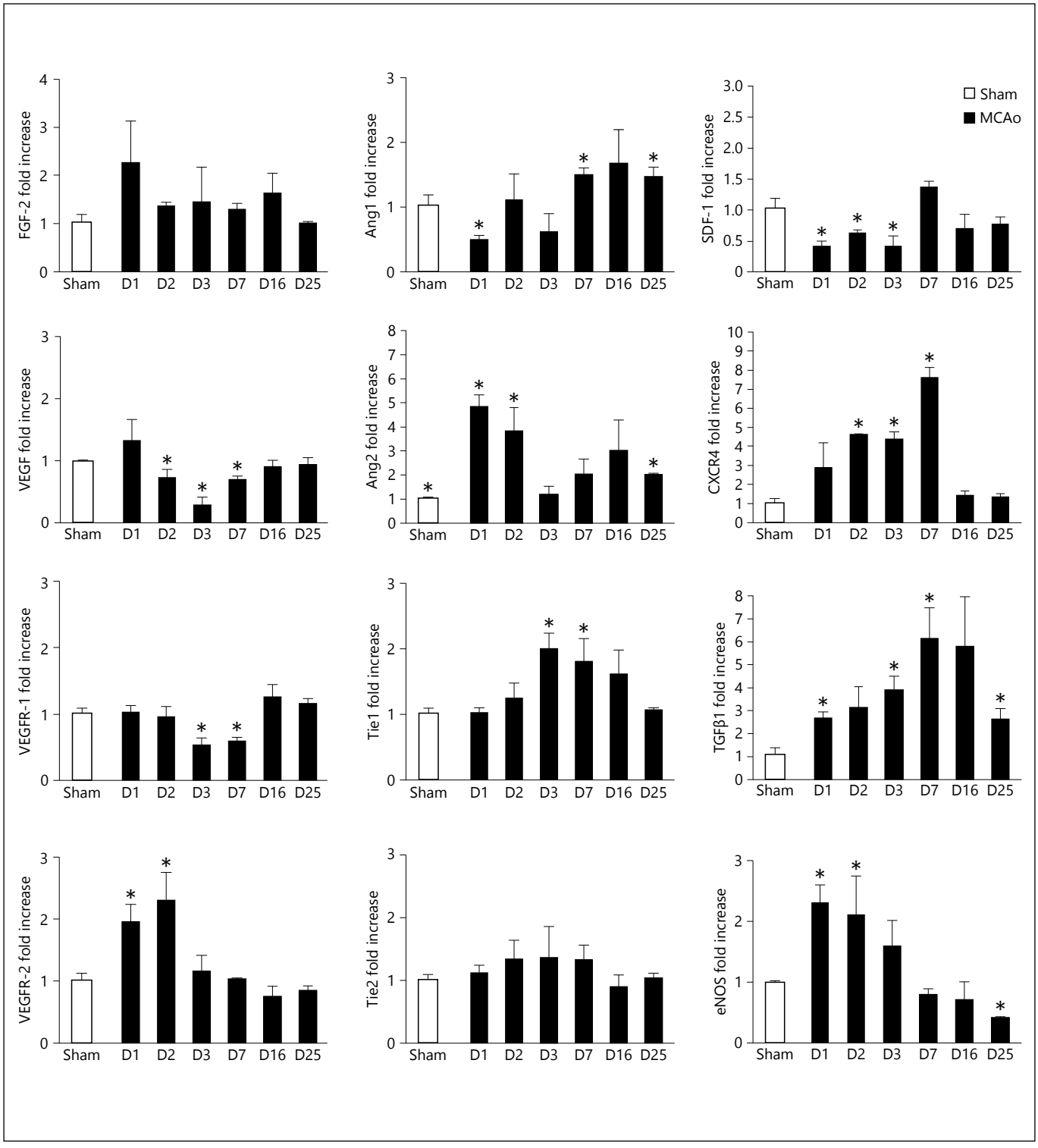

Fig. 3. Follow-up of the brain expression of 12 factors after middle cerebral artery occlusion (MCAo). The quantitative values are expressed as ratios of factors mRNA between MCAo and sham rats (mean ratio ± SEM). * $p \leq 0.05$ (Mann-Whitney).

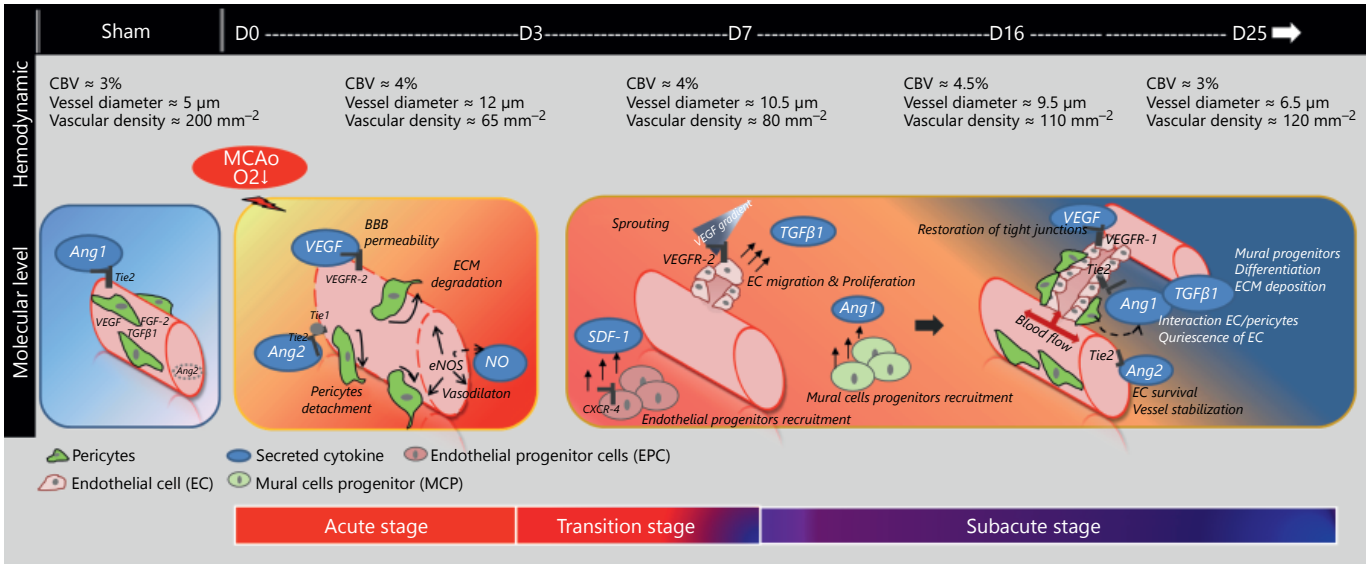

Fig. 4. Hemodynamic and molecular vascular events that occur during the acute (D1–D3), the transition (D3–D7) and the subacute (from D7) stages following a focal cerebral ischemia/reperfusion (middle cerebral artery occlusion, MCAo). In sham rats, vessels are stable and organized under the influence of Ang1. VEGF and TGFβ1 are stored in the extracellular matrix (ECM). Ang2 is stored in the Weibel–Palade bodies of endothelial cells (EC). In MCAo rats, at the 'acute stage' of stroke, hypoxia leads to the transcription of VEGF and eNOS that are consequently overexpressed in the damaged area. VEGF induces release of Ang2 from the Weibel-Palade bodies thus promoting pericyte detachment. The eNOS synthesizes NO that induces the vasodilation of preexisting vessels. Altogether these events take part to the hyperpermeability of the blood brain barrier, induced by VEGF through the activation of its receptor VEGFR-2, and to the destabilization of vessels. At D3 after stroke, the CBV is increased because of the large vasodilation. During the 'transition stage', the VEGF released from the degraded ECM targets the EC where sprouting occurs through activation of VEGFR-2. TGFβ1 (low level) acts as a chemokine to guide the migration of the sprouting new vessel toward the damaged area. In parallel, SDF-1 acts as a chemokine to recruit the endothelial progenitor cells from the bone. Ang1 is responsible for the recruitment of mural cells progenitors from the bone marrow. At the 'subacute stage', TGFβ1 is responsible for the deposition of ECM around new vessels and differentiation of mural progenitors in pericytes. In conjunction with Ang1, it also promotes interactions between EC and pericytes and favors the quiescence/survival of EC. Ang2 promotes EC survival and participates to the stabilization of vessels.

pression were first higher (Ang2) or similar (VEGF, VEGFR-1) to sham during the first 2 days, dropped at D3, and rose again from D16.

The expression of the seven other factors showed a bell-shape evolution. The maximum ratio was observed at the first stage for VEGFR-2 (D2) and eNOS (D1), at the second stage for TGFβ1 and Ang1 (D7–D16), and between both stages for Tie1 (D3–D7), SDF-1, and CXCR-4 (D7).

Except for TGFβ1, Ang1, and Ang2, the expression of growth factors returned to the sham baseline level at D25.

Discussion

This study describes the microvascular plasticity at molecular and integrated levels in the same rat model during 25 days after stroke. Biological and MRI data (fig. 4) identify an acute and subacute stage with a molecular 'transition stage' in-between [4]. At each step, biological events precede by at least one day the microvascular changes observed by MRI.

Duality of the Acute Stage: BBB Permeability and Provision of a Pro-Angiogenic Microenvironment

We defined the 'acute stage' following cerebral ischemia between D1 and D3, where the functional deficit was the worst. We observed a decreased vascular density with increased CBV and vessel caliber (VSI) in conjunction with a major BBB permeability at D3. Similar evolutions of CBV and perfused vessel caliber have been reported in a three-vessel occlusion model [21] and in an MCAo model (transient 60 min) [24]. For BBB permeability, similar observations were obtained in an MCAo model (transient 90 min) [30]. In line with MRI, histology revealed enlarged and destabilized vessels (fig. 2) during this 'acute' phase.

MRI events observed at D3 could be consistent with the angiogenic factors expressed at D1 and D2 (increase in Ang2, eNOS, and VEGFR-2) rather than those expressed at D3 (decrease in Ang2, VEGF, and VEGFR-2, increase in Tie1, CXCR4, and TGFβ1). At D1 and D2, increases in Ang2, VEGF and VEGFR-2 have previously been reported in MCAo rats [9, 10]. These molecular events are known to be responsible for vasodilation, detachment of pericytes, and destabilization of vessels [31], which represent the first angiogenesis step [32]. Moreover, the overexpression of eNOS observed in this study is expected to major the stroke-induced vasodilation [33].

At D3, we observed a drop in the expression of Ang2, VEGF, and VEGFR-2, in line with previous reports [9, 10, 34]. In contrast, the expression of TGFβ1, Tie1, and CXCR-4 began to increase from D3. This molecular angiogenic pattern signs the 'transition stage' between the acute (D1–D3) and subacute (D7–D25) stages [4].

During the acute phase, a shift-in-time of about few days appeared between the molecular and microvascular events. The microvascular events at D3 are more in line with the molecular expression at D1 and D2, and the complex molecular expression pattern at D3 might indicate that transition to the subacute stage has already begun.

Subacute Stage, the Time for Vascular Maturation and Stabilization

The 'subacute stage' began from D7 following ischemic injury. The increased microvascular density associated with a decreased vessel caliber and BBB permeability (fig. 1a) confirms the occurrence of angiogenesis in the damaged hemisphere. These results are in line with Lin et al. and Strbian et al. [21, 30] but not with Boehm-Sturm et al. [24] who did not detect change in microvessel density or caliber. This discrepancy might be ascribed to difference in MRI methodology (use of multi-echo vs. single-echo to map change in T_2) or animal model (60- vs. 90-min transient MCAo). At the molecular level, the expression pattern of Ang1 is consistent with previous studies (permanent and 60 min MCAo) [10, 35]. Interestingly, these two studies describe a correlation between Ang1 overexpression, decreased histological vessel caliber, and enhanced vascular density at the subacute stage. In addition, Ang1 is known to restore the tight junctions between EC and thereby decrease the BBB permeability [36]. The strong overexpression of TGFβ1 (compared to acute stage) is known to induce the formation of ECM around new vessels and to promote the differentiation of mural progenitors in pericytes [37]. In conjunction with Ang1, TGFβ1 may also promote interactions between EC and pericytes [38, 39] and induce quiescence and survival of EC [40]. At this stage, quiescent EC express VEGFR-1 rather than VEGFR-2, to avoid new sprouting events [31]. The second peak of Ang2, observed at D16, has been reported after 60-min MCAo in rats but not in a 30-min MCAo model in mice [10, 16]. At this stage, Ang2 may promote EC survival [41] and participate to vascular stabilization [42]. Altogether, these molecular events corroborate well the MRI observations. Microvessel stabilization is also suggested by our histological data (fig. 2).

At D25, the vascular density failed to reach the sham level despite a CBV comparable to that of sham animals. At a molecular level, angiogenic factors are either comparable to that of sham following a trend toward normal values. This suggests a slowdown of the microvascular plasticity. The lower vascular density obtained at D25 might limit the response to the metabolic demand of tissue. In line with the concept of neurovascular unit and the role of several angiogenic factors in neurogenesis, the new microvasculature could be insufficient to prevent the premature death of neurons [43, 44]. From a therapeutic point of view, it could be of interest to enhance the vascular remodeling and vessel formation during this subacute phase notably using cell-based therapy [45, 46].

Conclusion

This study describes the microvascular plasticity after cerebral ischemia at molecular and integrated levels. The 'acute stage' (D1–D3) is characterized by high levels of Ang2, VEGFR-2, and eNOS that altogether may be associated with deleterious BBB permeability and vasodilation. The 'transition stage' (D3–D7) involves TGFβ1, Ang1, Tie1, SDF-1, and CXCR-4. The 'subacute stage' takes place after D7 and is characterized by high levels of Ang1, Ang2, VEGF, VEGFR-1, and TGFβ1 that may lead to favorable stabilization and maturation of vessels. Further investigations are needed to detail the mechanisms responsible for these angiogenic events and to assess the link between microvascular remodeling, MRI observations, and behavioral improvements. All MRI parameters varied over time, revealing the different aspects of the microvascular plasticity. This suggests that multiparametric MRI can provide interesting biomarkers to assess angiogenesis after stroke. At D25, despite a normal CBV, MRI revealed a limited microvessel density, which might be insufficient to support a good neural repair. Thus, pro-

angiogenic neurorestorative therapies would be relevant notably during the subacute phase of stroke when endogenous vessel maturation and stabilization occur.

Acknowledgments

Guerbet Lab. (France) for providing contrast agent P904®. Animal facility technicians of Grenoble Institute of Neurosciences for providing technical support. Grenoble MRI facility IRMaGe was partly funded by the French program 'Investissement d'Avenir' run by the 'Agence Nationale pour la Recherche'; grant 'Infrastructure d'avenir en Biologie Santé' – ANR-11-INBS-0006.

Disclosure Statement

No conflict of interest.

References

1 Mead GE, Hsieh CF, Lee R, Kutlubaev M, Claxton A, Hankey GJ, Hackett M: Selective serotonin reuptake inhibitors for stroke recovery: a systematic review and meta-analysis. Stroke 2013;44:844–850.

2 Dirnagl U, Iadecola C, Moskowitz MA: Pathobiology of ischaemic stroke: an integrated view. Trends Neurosci 1999;22:391–397.

3 Arai K, Lok J, Guo S, Hayakawa K, Xing C, Lo EH: Cellular mechanisms of neurovascular damage and repair after stroke. J Child Neurol 2011;26:1193–1198.

4 Arai K, Jin G, Navaratna D, Lo EH: Brain angiogenesis in developmental and pathological processes: neurovascular injury and angiogenic recovery after stroke. FEBS J 2009;276:4644–4652.

5 Liman TG, Endres M: New vessels after stroke: postischemic neovascularization and regeneration. Cerebrovasc Dis 2012;33:492–499.

6 Krupinski J, Kaluza J, Kumar P, Kumar S, Wang JM: Role of angiogenesis in patients with cerebral ischemic stroke. Stroke 1994;25:1794–1798.

7 Onda T, Honmou O, Harada K, Houkin K, Hamada H, Kocsis JD: Therapeutic benefits by human mesenchymal stem cells (hMSCs) and Ang-1 gene-modified hMSCs after cerebral ischemia. J Cereb Blood Flow Metab 2008;28:329–340.

8 Palmer TD, Willhoite AR, Gage FH: Vascular niche for adult hippocampal neurogenesis. J Comp Neurol 2000;425:479–494.

9 Hayashi T, Noshita N, Sugawara T, Chan PH: Temporal profile of angiogenesis and expression of related genes in the brain after ischemia. J Cereb Blood Flow Metab 2003;23:166–180.

10 Lin TN, Wang CK, Cheung WM, Hsu CY: Induction of angiopoietin and Tie receptor mRNA expression after cerebral ischemia-reperfusion. J Cereb Blood Flow Metab 2000;20:387–395.

11 Baranova O, Miranda LF, Pichiule P, Dragatsis I, Johnson RS, Chavez JC: Neuron-specific inactivation of the hypoxia inducible factor 1 alpha increases brain injury in a mouse model of transient focal cerebral ischemia. J Neurosci 2007;27:6320–6332.

12 Fan Y, Shen F, Frenzel T, Zhu W, Ye J, Liu J, Chen Y, Su H, Young WL, Yang GY: Endothelial progenitor cell transplantation improves long-term stroke outcome in mice. Ann Neurol 2010;67:488–497.

13 Planas AM, Sole S, Justicia C: Expression and activation of matrix metalloproteinase-2 and -9 in rat brain after transient focal cerebral ischemia. Neurobiol Dis 2001;8:834–846.

14 Hu M, Zhang X, Liu W, Cui H, Di N: Longitudinal changes of defensive and offensive factors in focal cerebral ischemia-reperfusion in rats. Brain Res Bull 2009;79:371–375.

15 Lin TN, Te J, Lee M, Sun GY, Hsu CY: Induction of basic fibroblast growth factor (bFGF) expression following focal cerebral ischemia. Brain Res Mol Brain Res 1997;49:255–265.

16 Lennmyr F, Terent A, Syvanen AC, Barbany G: Vascular endothelial growth factor gene expression in middle cerebral artery occlusion in the rat. Acta Anaesthesiol Scand 2005;49:488–493.

17 Slevin M, Krupinski J, Rovira N, Turu M, Luque A, Baldellou M, Sanfeliu C, de Vera N, Badimon L: Identification of pro-angiogenic markers in blood vessels from stroked-affected brain tissue using laser-capture microdissection. BMC Genomics 2009;10:113.

18 Ohab JJ, Fleming S, Blesch A, Carmichael ST: A neurovascular niche for neurogenesis after stroke. J Neurosci 2006;26:13007–13016.

19 Beck H, Plate KH: Angiogenesis after cerebral ischemia. Acta Neuropathol 2009;117:481–496.

20 Xu C, Schmidt WU, Villringer K, Brunecker P, Kiselev V, Gall P, Fiebach JB: Vessel size imaging reveals pathological changes of microvessel density and size in acute ischemia. J Cereb Blood Flow Metab 2011;31:1687–1695.

21 Lin CY, Chang C, Cheung WM, Lin MH, Chen JJ, Hsu CY, Chen JH, Lin TN: Dynamic changes in vascular permeability, cerebral blood volume, vascular density, and size after transient focal cerebral ischemia in rats: evaluation with contrast-enhanced magnetic resonance imaging. J Cereb Blood Flow Metab 2008;28:1491–1501.

22 Bosomtwi A, Jiang Q, Ding GL, Zhang L, Zhang ZG, Lu M, Ewing JR, Chopp M: Quantitative evaluation of microvascular density after stroke in rats using MRI. J Cereb Blood Flow Metab 2008;28:1978–1987.

23 Ding G, Jiang Q, Li L, Zhang L, Zhang ZG, Ledbetter KA, Gollapalli L, Panda S, Li Q, Ewing JR, Chopp M: Angiogenesis detected after embolic stroke in rat brain using magnetic resonance T2*WI. Stroke 2008;39:1563–1568.

24 Boehm-Sturm P, Farr TD, Adamczak J, Jikeli JF, Mengler L, Wiedermann D, Kallur T, Kiselev V, Hoehn M: Vascular changes after stroke in the rat: a longitudinal study using optimized magnetic resonance imaging. Contrast Media Mol Imaging 2013;8:383–392.

25 Moisan A, Pannetier N, Grillon E, Richard MJ, de Fraipont F, Remy C, Barbier EL, Detante O: Intracerebral injection of human mesenchymal stem cells impacts cerebral microvasculature after experimental stroke: MRI study. NMR Biomed 2012;25:1340–1348.

26 Detante O, Moisan A, Dimastromatteo J, Richard MJ, Riou L, Grillon E, Barbier EL, Desruet MD, de Fraipont F, Segebarth C, Jaillard A, Hommel M, Ghezzi C, Remy C: Intravenous administration of 99mTc-HMPAO-labeled human mesenchymal stem cells after stroke: in vivo imaging and biodistribution. Cell Transplant 2009;18:1369–1379.

27 Detante O, Valable S, de Fraipont F, Grillon E, Barbier E, Moisan A, Arnaud J, Moriscot C, Segebarth C, Hommel M, Remy C, Richard MJ: Magnetic resonance imaging and fluorescence labeling of clinical-grade mesenchymal stem cells without impacting their phenotype: study in a rat model of stroke. Stem Cells Transl Med 2012;1:333–341.

28 Wu EX, Tang H, Jensen JH: High-resolution MR imaging of mouse brain microvasculature using the relaxation rate shift index Q. NMR Biomed 2004;17:507–512.

29 Schmittgen TD, Livak KJ: Analyzing real-time PCR data by the comparative C(T) method. Nat Protoc 2008;3:1101–1108.

30 Strbian D, Durukan A, Pitkonen M, Marinkovic I, Tatlisumak E, Pedrono E, Abo-Ramadan U, Tatlisumak T: The blood-brain barrier is continuously open for several weeks following transient focal cerebral ischemia. Neuroscience 2008;153:175–181.

31 Potente M, Gerhardt H, Carmeliet P: Basic and therapeutic aspects of angiogenesis. Cell 2011;146:873–887.

32 Pettersson A, Nagy JA, Brown LF, Sundberg C, Morgan E, Jungles S, Carter R, Krieger JE, Manseau EJ, Harvey VS, Eckelhoefer IA, Feng D, Dvorak AM, Mulligan RC, Dvorak HF: Heterogeneity of the angiogenic response induced in different normal adult tissues by vascular permeability factor/vascular endothelial growth factor. Lab Invest 2000; 80:99–115.

33 Cuevas P, Garcia-Calvo M, Carceller F, Reimers D, Zazo M, Cuevas B, Munoz-Willery I, Martinez-Coso V, Lamas S, Gimenez-Gallego G: Correction of hypertension by normalization of endothelial levels of fibroblast growth factor and nitric oxide synthase in spontaneously hypertensive rats. Proc Natl Acad Sci U S A 1996;93:11996–12001.

34 Zan L, Wu H, Jiang J, Zhao S, Song Y, Teng G, Li H, Jia Y, Zhou M, Zhang X, Qi J, Wang J: Temporal profile of Src, SSeCKS, and angiogenic factors after focal cerebral ischemia: correlations with angiogenesis and cerebral edema. Neurochem Int 2011;58:872–879.

35 Beck H, Acker T, Wiessner C, Allegrini PR, Plate KH: Expression of angiopoietin-1, angiopoietin-2, and tie receptors after middle cerebral artery occlusion in the rat. Am J Pathol 2000;157:1473–1483.

36 Valable S, Montaner J, Bellail A, Berezowski V, Brillault J, Cecchelli R, Divoux D, Mackenzie ET, Bernaudin M, Roussel S, Petit E: VEGF-induced BBB permeability is associated with an MMP-9 activity increase in cerebral ischemia: both effects decreased by Ang-1. J Cereb Blood Flow Metab 2005;25:1491–1504.

37 Pepper MS, Belin D, Montesano R, Orci L, Vassalli JD: Transforming growth factor-beta 1 modulates basic fibroblast growth factor-induced proteolytic and angiogenic properties of endothelial cells in vitro. J Cell Biol 1990;111:743–755.

38 Lebrin F, Deckers M, Bertolino P, Ten Dijke P: TGF-beta receptor function in the endothelium. Cardiovasc Res 2005;65:599–608.

39 Gaengel K, Genove G, Armulik A, Betsholtz C: Endothelial-mural cell signaling in vascular development and angiogenesis. Arterioscler Thromb Vasc Biol 2009;29:630–638.

40 Goumans MJ, Valdimarsdottir G, Itoh S, Rosendahl A, Sideras P, ten Dijke P: Balancing the activation state of the endothelium via two distinct TGF-beta type I receptors. EMBO J 2002;21:1743–1753.

41 Kim I, Kim JH, Moon SO, Kwak HJ, Kim NG, Koh GY: Angiopoietin-2 at high concentration can enhance endothelial cell survival through the phosphatidylinositol 3′-kinase/Akt signal transduction pathway. Oncogene 2000;19:4549–4552.

42 Teichert-Kuliszewska K, Maisonpierre PC, Jones N, Campbell AI, Master Z, Bendeck MP, Alitalo K, Dumont DJ, Yancopoulos GD, Stewart DJ: Biological action of angiopoietin-2 in a fibrin matrix model of angiogenesis is associated with activation of Tie2. Cardiovasc Res 2001;49:659–670.

43 Arvidsson A, Collin T, Kirik D, Kokaia Z, Lindvall O: Neuronal replacement from endogenous precursors in the adult brain after stroke. Nat Med 2002;8:963–970.

44 Greenberg DA, Jin K: Vascular endothelial growth factors (VEGFs) and stroke. Cell Mol Life Sci 2013;70:1753–1761.

45 Gutierrez M, Merino JJ, Alonso de Lecinana M, Diez-Tejedor E: Cerebral protection, brain repair, plasticity and cell therapy in ischemic stroke. Cerebrovasc Dis 2009;27(suppl 1): 177–186.

46 Onteniente B, Polentes J: Regenerative medicine for stroke – are we there yet? Cerebrovasc Dis 2011;31:544–551.